Analyzing Optimal Operating Points of Air and Water-Cooled Chillers Used in an Office Building

Felipe Yagi Ng[1] , Caique dos Santos[1] , Catarina Gomes dos Santos[1] ,
Maria Thereza de Moraes Gomes Rosa[2] , and Míriam Tvrzská de Gouvêa[1(✉)]

[1] School of Engineering, Mackenzie Presbyterian University, São Paulo, Brazil
miriamtg_br@yahoo.com
[2] Science and Technology Centre, Mackenzie Presbyterian University, Campinas, Brazil

Abstract. With the huge development of big cities, there was an increase in the number of large buildings used for commercial and administrative purposes and, as a result, the need to use air conditioning systems with lower energy consumption and that guarantee thermal comfort. Air-water-type air conditioning systems are commonly used. In order to operate those conditioning systems, air or water-cooled chillers are used. In this work, a mathematical effectiveness model is used to represent the thermal behavior of a forced circulation cooling tower, which was incorporated into the existing chiller's model of the simulator of Edifício Moderno, enabling the optimization of the operation of both air and water-cooled chiller. Hence, the optimal operating points of both types of chillers are compared. Two different objective functions are used in optimization problems. Simulation results show a reduction of at least 14% in the energy consumed when the air condenser is replaced with the water condenser. Moreover, manipulated variables vary less to control the operation of water-cooled chillers. The optimization problems were easily solved and can be used not only to optimize the operation of the air conditioning system but also to understand the operation of chillers.

Keywords: Air-water conditioning systems · Cooling tower · Optimization

1 Introduction

Large commercial and administrative buildings are present nowadays in large cities and require energy-demanding air conditioning systems to ensure thermal comfort. Thus, thermally efficient operation of air conditioning systems is an utmost need. The vast majority of air conditioning systems use a vapor compression system to remove the thermal load from the building, rejecting it into the environment. According to [1], in air-water-type air conditioning systems, widely used in large buildings that aim thermal comfort, air or water-cooled chillers are used to produce chilled water that will promote the conditioning of the zones. In air-cooled chillers, the condenser of the steam compression system uses ambient air as a cooling fluid and in water-cooled chillers, condensers use cold water as a cooling fluid, which is cooled with ambient air in a cooling tower.

A simulator was developed in MATLAB® for the air conditioning system of Edifício Moderno by [2], which is a virtual building based on a real large commercial building, used primarily for offices, located in Belo Horizonte, Minas Gerais, Brazil. Its air-water-type air conditioning system covers an area of 19193 m². In the simulator developed by [2] and further modified by [3], an air-cooled chiller was considered. In this work, a model of a water-cooled condenser with a cooling tower is incorporated into the simulator, which allows performing studies of the behavior of air and water chillers in air conditioning systems under different environmental conditions and heat loads. The air conditioning system operating with a water-cooled condenser considered in this work is schematically shown in Fig. 1. In this paper, we focus on the steady-state optimization of the operation of one of the three chillers used to produce cold water to condition the 298 zones of the building. Recently, it has been of interest not to neglect the energy consumption of the fans of the cooling tower or air condensers [4]. Despite this interest, there are still few publications dealing with the integrated energy optimization of steam compression systems, as done in this work.
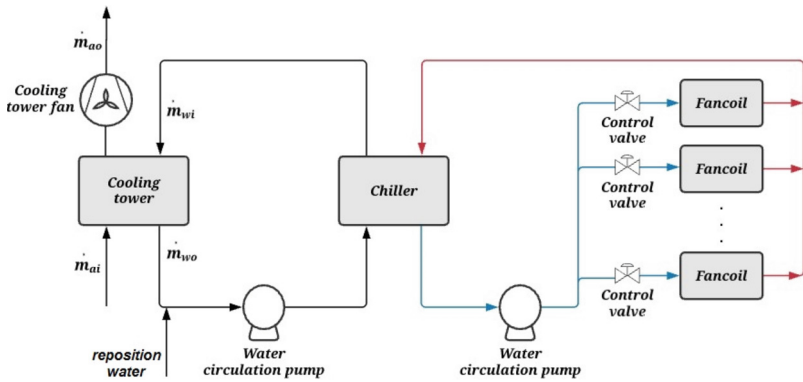

Fig. 1. Typical installation of the water-cooled chiller in an air-water air conditioning system.

2   Description of the Mathematical Model of the Cooling Tower

The tower model that was integrated into the simulator of the air conditioning system of Edifício Moderno is based on the effectiveness model proposed by [5], which considers the occurrence of heat and mass transfer solely in the direction normal to the air and water flows and also assumes the constant temperature of the water stream in each cross-section of the tower. Despite these assumptions, it is shown to adequately predict the operation of real cooling towers [5, 6]. The effectiveness is defined as the ratio between the actual heat transfer and the maximum possible heat transfer so that the heat exchanged between air and water in the cooling tower is given by the model of [5] in Eq. 1, where $\dot{Q}$ represents the heat transfer between water and air in the cooling tower, ε_a is the effectiveness of the cooling tower, $\dot{m}_{ai}$ is mass flow of air introduced into the

cooling tower, h_{swi} is the air saturation enthalpy at the inlet water temperature T_{wi}, and h_{ai} is the enthalpy of air entering the cooling tower.

$$\dot{Q} = \varepsilon_a \dot{m}_{ai}(h_{swi} - h_{ai}) \tag{1}$$

The effectiveness of the tower is determined by Eq. 2, in which the effective air-water capacitance ratio m^* is calculated accordingly to Eq. 3, and the number of transfer units NTU is obtained as a function of empirical constants c and n as shown in Eq. 4. These constants depend on the constructive form and design characteristics of each tower. In this work, we selected them from the available values in the literature [5, 6], which enabled good reproduction of the data in the datasheet of the cooling tower used in this work, so that, $c = 2.3$ and $n = -0.72$ in this work. In Eq. 3, c_w is the specific heat of liquid water, c_s is the air saturated heat capacity predicted from the saturation linearized enthalpy gradient accordingly to Eq. 5, and $\dot{m}_{wi}$ is the mass flow rate of water at the entrance of the cooling tower. In Eq. 5, h_{swo} is air saturation enthalpy at water temperature leaving the cooling tower, and T_{wo} indicates the cooling tower water outlet temperature.

$$\varepsilon_a = \frac{1 - e^{-NTU(1-m^*)}}{1 - m^* e^{-NTU(1-m^*)}} \tag{2}$$

$$m^* = \frac{\dot{m}_{ai}}{\dot{m}_{wi}} \frac{c_w}{c_s} \tag{3}$$

$$NTU = c \left(\frac{\dot{m}_{wi}}{\dot{m}_{ai}} \right)^{1+n} \tag{4}$$

$$c_s = \left(\frac{\partial h_s}{\partial T} \right)\bigg|_{T=T_w} = \frac{h_{swi} - h_{swo}}{T_{wi} - T_{wo}} \tag{5}$$

Exit air enthalpy h_{ao} and water exit temperature are calculated, respectively, by Eqs. 6 and 7. Note that Eq. 7 assumes that there is a loss of water through evaporation. Air saturation enthalpies are predicted considering the ASHRAE models [7]. In Eq. 7, $\dot{m}_{wo}$ is the water mass flow rae exiting the cooling tower.

$$h_{ao} = h_{ai} + \varepsilon_a(h_{swi} - h_{ai}) \tag{6}$$

$$T_{wo} = \frac{\dot{m}_{wi}c_w T_{wi} + \dot{m}_{ai}(h_{ai} - h_{ao})}{\dot{m}_{wo}c_w} \tag{7}$$

The prediction of water loss by evaporation is modeled by Eqs. 8 and 9, following the approach of [5]. The absolute humidity UA_{swe} is obtained from the saturation enthalpy evaluated by Eq. 10 and relative humidity of 100%. In Eq. 8, UA_o is absolute air humidity at the outlet of the cooling tower, UA_i is absolute air humidity at the inlet to the cooling tower and UA_{swe} is the absolute air humidity at the water outlet temperature at the point of greatest efficiency of the cooling tower. In Eq. 10, h_{swe} is the air saturation enthalpy at water outlet temperature at the point of greatest efficiency of the cooling tower.

$$UA_o = UA_i + (UA_i - UA_{swe})e^{-NTU} \tag{8}$$

$$\dot{m}_{wo} = \dot{m}_{wi} - \dot{m}_{ai}(UA_o - UA_i) \tag{9}$$

$$h_{swe} = h_{ai} + \frac{h_{ao} - h_{ai}}{1 - e^{-NTU}} \tag{10}$$

Since there is a loss of water due to evaporation, one last heat balance must be incorporated into the process model, which is shown in Eq. 11, where T_{wr} and T_{ci}, are, respectively, the temperatures of the reposition water and the water entering the condenser of the chiller. Note that the heat capacity of liquid water is constant [7].

$$T_{ci} = \frac{\dot{m}_{wo}T_{wo} + (\dot{m}_{wi} - \dot{m}_{wo})T_{wr}}{\dot{m}_{wi}} \tag{11}$$

3 Simulation Results

The nominal operating points of both types of chillers were obtained by applying the following procedure. First, superheating, subcooling, and the evaporator's heat duty were fixed, respectively at 5 °C, 0.5 °C, and 1064.4 kW. External air's dry and wet bulb temperatures were considered to be 32 °C and 24 °C. For the water-cooled chiller, the temperature of water at the exit of the condenser was also fixed to 35 °C. Hence, there were no degrees of freedom left for optimization and the chiller model was solved. For solving the system of nonlinear algebraic equations with 23 decision variables for the water-cooled chiller and 19 decision variables for the air-cooled chiller, the SQP optimization method was selected using the *fmincon* function of MATLAB®.

A constant objective function equal to 2 was used for that purpose. The model was simulated using MATLAB® R2006b, running on a 32bit Centrino Dual Intel processor. All simulations performed in this work took less than 1 s. The obtained solution was then considered as the initial point for solving an optimization problem that aimed to minimize only the power consumption of the compressor. For the optimization problem, just the heat duty was fixed and again the SQP method was used to solve the optimization problem. Lower bounds for superheating and subcooling were considered as 5 °C and 0.5 °C.

The solution obtained after this procedure is considered as the nominal operating point in this work and is presented in Table 1, where it is labeled as case *n*. It is noteworthy to say that nominal values for the temperature and flow rate of water into the evaporator are, respectively, 12.2 °C and 46.62 kg/s. The equations that describe the compressor, condenser, and electronic expansion valve can be found in [2] and the evaporator model is described in [3]. The latter consists of a rigorous model of a TEMA shell and tubes heat exchanger and both the superheating and two-phase flow regions are modeled. In this work, we did not vary the temperature of the water exiting the evaporator. Hence, for all simulation water exits the evaporator at the nominal operating point of the air conditioning system of Edifício Moderno, namely, 6.7 °C. The temperature of reposition water was kept constant at 26 °C in all simulations.

Besides the nominal operating point, in Table 1, two other sets of simulation results are presented. The model of the condenser considered in this work is dependent on the

nominal design value of the global heat exchange coefficient. So, in order to analyze the effect of changes in the value of the product of the global heat exchange coefficient by heat exchange area, in case S1, the nominal value was increased for both air and water-cooled chillers to 160 kW/K. In simulation case S2, the objective function of the optimization problem was changed to minimize both external air flowrate and compressor's work, according to Eq. 12 for the water-cooled chiller and Eq. 13 for the air-cooled chiller. In Eq. 12, $\dot{W}_{cp}$ is the power of the compressor, $\dot{V}_{ai}$ and VU_{ai} are, respectively, the volumetric flow rate of air into the tower or condenser and the ambient specific humid volume of air. In Table 1, ω, A_{eev}, P_{cpo}, P_{cpi}, T_{cpi}, T_{cpo}, $\dot{m}_{rf}$, T_{ci}, T_{co}, are, respectively, the compressor speed, the opening of the electronic expansion valve, the outlet and inlet pressure of the compressor, the inlet and outlet temperature of the compressor, the mass flow rate of refrigerant in the vapor compression cycle and the temperatures of the cold fluid at the entry and exit of the condenser. Note that for the water-cooled condenser $T_{co} = T_{wi}$.

$$\dot{W}_{cp} + 2 \times 10^{-5} \left(\frac{\dot{V}_{ai}}{VU_{ai}} \right)^3 \tag{12}$$

$$\dot{W}_{cp} + 4, 4 \times 10^{-5} \dot{V}_{ai}^3 \tag{13}$$

Table 1. Nominal operating point of air and water-cooled chillers.

Chiller-simulation case	$\dot{W}_{cp}$ (kW)	$\dot{V}_{ai}$ (m³/s)	ω (Hz)	A_{eev} (%)	$\frac{P_{cpo}}{P_{cpi}}$	T_{cpi} (°C)	T_{cpo} (°C)	$\dot{m}_{rf}$ (kg/s)	T_{ci} (°C)	T_{co} (°C)
w − n	295.5	26.4	34.6	27.2	4.35	1.5	90.6	5.27	30.7	34.5
w − S1	295.5	16.2	34.6	27.2	4.35	1.5	90.6	5.27	31.9	40.4
w − S2	295.5	15.1	34.6	27.2	4.35	1.5	90.6	5.27	36.4	39.0
air − n	365.2	137.1	42.7	46.4	4.33	1.6	90.6	6.53	32	40.9
air − S1	343.7	137.1	40.2	39.5	4.33	1.6	90.6	6.14	32	40.8
air − S2	391.7	107.0	45.8	57.0	4.33	1.6	90.5	7.01	32	43.7

The results in Table 1 show that, for all scenarios for the water-cooled chiller, the same operation point for the refrigerant side is obtained regardless of the condenser global heat exchange coefficient or the water flow rate and state values into the condenser. However, different operating points for the cooling tower are predicted. Implicit to this observation is the fact that multiple minimum points exist. For the water-cooled chiller, minimum bounds on superheating and the temperature of the refrigerant leaving the condenser are reached. For the air-cooled chiller, significantly different behavior is observed.

For the nominal and S1 cases, maximum bound on the external air flow rate and minimum superheating are reached and the operation of the chiller is dependent on the heat capacity of the condenser. Although the compression ratios are quite similar for both chillers, the power consumed by the air-cooled chiller is much larger. If the

external air flow rate into the condenser is also minimized, the power of the compressor increases only for the air-cooled chiller. Hence, the operation of the air-cooled chiller is much more dependent on external air condition than the water-cooled chiller. Another interesting result is that the opening of the electronic expansion valve (EEV) is smaller for the water-cooled chiller and the percentage of the opening varies significantly among the simulated cases for the air-cooled chiller but much less for the water-cooled chiller.

Tables 2 and 3 show simulation scenarios related to perturbations in external ambient conditions or the heat load of the evaporator. For all these simulations the optimization problems were formulated using Eq. 13 as the objective function for the air-cooled chiller and Eq. 12 for the water-cooled chiller. As expected, the minimum superheating constraint was hit in all simulations. In Table 2, $\dot{Q}_{ev}$, $\dot{m}_{we}$, T_{wei}, $\dot{m}_{loss}$, UR_i, UR_o stand for the heat duty of the evaporator, water flow rate and temperature from building into the evaporator, water loss due to evaporation in the cooling tower, relative humidity of ambient air, and of leaving air from cooling tower. Note that the same perturbations are made for both chillers and that in Table 3 T_{ai} and UR_i indicate the inlet air conditions into the air condenser or into the cooling tower.

Table 2. Perturbations applied and optimal operating point for cooling tower.

Chiller - perturbation	$\dot{Q}_{ev}$ (kW)	$\dot{m}_{we}$ (kg/s)	T_{wei} (°C)	T_{ai} (°C)	UR_i (%)	$\dot{m}_{wi}$ (kg/s)	$\dot{m}_{loss}$ (kg/s)	T_{ao} (°C)	UR_o (%)
w – P1	870.9	46.62	11.2	33	50	124.3	0.409	41.1	99.7
w – P2	1064.4	46.62	12.2	33	50	124.3	0.510	38.7	99.4
w – P3	1257.9	46.62	13.2	33	50	124.3	0.621	36.2	98.9
w – P4	1295.7	48.02	13.2	33	50	124.3	0.645	35.8	98.9
w – P5	870.9	46.62	11.2	30	80	124.3	0.388	41.0	100
w – P6	1064.4	46.62	12.2	30	80	124.3	0.478	38.5	99.7
w – P7	1257.9	46.62	13.2	30	80	124.3	0.572	36.4	98.7
w – P8	870.9	46.62	11.2	30	50	124.3	0.399	41.1	99.9

In regard to the water-cooled chiller, simulation results in Table 3 show similar behavior as observed previously for simulation results in Table 1, namely, the heat load of the evaporator sets the operating point for the refrigerant size of the chiller. It is a noteworthy fact that, for all simulations, the water flow rate into the condenser of the water-cooled chiller reached its upper bound limit. The main difference in the operating points is related to the flow rate of air into the cooling tower. The higher the heat load of the evaporator, the larger the flow rate, as expected. Although air temperature of external air in perturbations P5 to P7 is lower than in perturbations P1 to P3, the relative humidity is very high and so the external air enthalpy is larger for cases P5 to P7 than for cases P1 to P3. That is why the air flow rates into the cooling tower are higher. Again, we can see that the optimal operating point of the water-cooled chiller is more sensitive to external air perturbations and that much more energy is consumed.

Table 3. Optimal operating point of air and water-cooled chillers.

Chiller - simulation	$\dot{W}_{cp}$ (kW)	$\dot{V}_{ai}$ (m³/s)	ω (Hz)	Aeev (%)	$\dfrac{P_{cpo}}{P_{cpi}}$	T_{cpi} (°C)	T_{cpo} (°C)	$\dot{m}_{rf}$ (kg/s)	T_{ci} (°C)	T_{co} (°C)
w – P1	234.8	10.1	26.8	22.4	4.19	2.8	90.0	4.30	39.2	41.3
w – P2	295.5	15.6	34.6	27.2	4.35	1.5	90.6	5.27	36.4	39.0
w – P3	360.3	24.0	43.4	32.2	4.53	0.1	91.3	6.24	33.6	36.7
w – P4	373.8	26.2	45.2	33.2	4.57	0.1	91.5	6.43	33.1	36.3
w – P5	234.8	11.4	26.8	22.4	4.19	2.8	90.0	4.30	38.0	41.3
w – P6	295.5	18.2	34.6	27.2	4.35	1.5	90.6	5.27	36.4	39.0
w – P7	360.3	29.7	43.4	32.2	4.53	0.1	91.3	6.24	33.6	36.7
w – P8	234.8	9.1	26.8	22.4	4.19	2.8	90.0	4.30	39.2	41.3
air – P1	294.8	87.4	33.6	38.5	4.16	3.0	90.0	5.42	33	41.3
air – P2	381.3	103.7	52.8	44.6	4.33	1.6	90.5	6.82	33	41.8
air – P3	477.9	120.3	57.5	75.3	4.53	0.2	91.3	8.28	33	42.3
air – P4	514.7	132.7	62.3	100	4.58	0.2	91.5	8.85	33	44.7
air – P5	306.4	91.5	34.9	42.5	4.16	3.0	90.0	5.64	30	44.1
air – P6	397.1	108.8	46.4	59.6	4.33	1.6	90.5	7.10	30	44.5
air – P7	498.8	126.5	60.0	93.6	4.53	0.1	91.3	8.64	30	44.9
air – P8	294.8	87.5	33.6	38.5	4.16	3.0	90.0	5.42	30	41.3

Variations in the manipulated variables (opening of the EEV, external air flow rate, and compressor's speed) are much more significant. However, there are also some resemblances between the operation points of both types of chillers. Compression ratios and entry and exit temperatures of the compressor are relatively similar. This is because the same compressor, evaporator, and electronic expansion valve are used for both chillers.

When comparing the operation of the two chillers, the water-cooled chiller should definitely be used if space limitations do not exist or if there are no constraints related to the need of replacing water for the cooling tower. Note that not only energy is saved when using water-cooled chillers, but also, controlling the operation of the environments within the building is expected to be less difficult because no manipulated variables reached their bounds for the water-cooled chiller, except the water flow rate through the condenser. The air-cooled chiller requires larger movements in the manipulated variables to control the operation and depending on the existing disturbances, the process is driven close to its operating limits, which might hinder controlling the temperatures of the zones within the building. Finally, the optimal operation of the chiller is easily obtained by applying the SQP optimization method and optimization should be definitely incorporated into control problems of air conditioning systems.

4 Conclusions

Simulation results show that the proposed model reproduces the expected behavior of air and water-cooled chillers. The effect of disturbances was also readily obtained. The optimization problems were easily and rapidly solved. Hence, exploring optimization problems can be not only used to optimize the operation but also to understand the operation. If there is not any space or water supply limitation, a water-cooled chiller should be used, not only because less energy is consumed during the operation of the chiller but also because fewer manipulations are required to control the exit water temperature of the evaporator.

References

1. De Araújo, N.M.: Estudo comparativo do projeto de um sistema VRF com um sistema ar-água para o condicionamento de ar em um edifício comercial de grande porte. Monografia. Universidade Presbiteriana Mackenzie (2016)
2. Pellegrini, R.L.S., de Araújo, N.M., de Gouvêa, M.T.: Modelling a water-air conditioning system of a large commercial building for energy consumption evaluation. In: Computer Aided Chemical Engineering, vol 44: Part C, pp. 1963–1968. Elsevier (2018)
3. Santos, C.G.; Ruivo, J.P.; Gasparini, L.B., Rosa, M.T.M.G.; Odloak, D. Tvrzská de Gouvêa, M.: Steady-state simulation and optimization of an air cooled chiller. Case Stud. Therm. Eng. (2022). https://authors.elsevier.com/tracking/article/details.do?aid=102142&jid=CSITE&surname=Tvrzsk%C3%A1+de+Gouv%C3%AAa
4. Lee, K.P., Cheng, T.: A simulation–optimization approach for energy efficiency of chilled water system. Energy Build. **54**, 290–296 (2012)
5. ASHRAE: Handbook of Fundamentals. ASHRAE Inc. (2017)
6. Braun, J.E., Klein, S.A., Mitchell, J.W.: Effectiveness models for cooling towers and cooling coils. Ashrae Trans. **2**, 164–174 (1989)
7. Liao, J., Xie, X., Nemer, H., Claridge, D.E., Culp, C.H.: A simplified methodology to optimize the cooling tower approach temperature control schedule in a cooling system. Energy Convers. Manage. **199**, 1–9 (2019)